Results in Nonlinear Analysis 8 (2025) No. 2, 8–27
https://doi.org/10.31838/rna/2025.08.02.002
Available online at www.nonlinear-analysis.com

Results in Nonlinear Analysis
ISSN 2636-7556

Peer Reviewed Scientific Journal

Bell Wavelet operational matrix method for convection diffusion equation

Shahid Ahmed[1], Bharti Yadav[2], Pooja Vats[2], Raksha Sharma*

[1]Department of Mathematics, Deen Dayal Upadhyaya College, University of Delhi, India; [2]School of Basic and Applied Sciences, K.R. Mangalam University, Gurugram, Haryana, India; [3]Department of Physics, Kirori Mal College, University of Delhi, Delhi, India

Abstract

In this article, we introduce an efficient method using Bell wavelets to solve fractional-order convection-diffusion equations with variable coefficients and initial-boundary conditions. We begin by integrating block pulse functions with the Bell wavelet matrix to construct the fractional-order operational matrix of integration (OMI). This method simplifies fractional models by converting them into a set of algebraic equations via the collocation technique. The Bell wavelet collocation technique results in an efficient computational approach characterised by low costs and rapid convergence. Four numerical examples are presented, and the results are compared with exact solutions and other existing methods to validate the method and demonstrate its effectiveness and applicability. Graphical results highlight significant variations between fractional and integer orders, while our method adeptly handles both initial and boundary conditions, enhancing overall accuracy and simple applicability.

Key words and phrases: Bell Wavelet, Fractional Derivative, Convection Diffusion Equation, Numerical Simulations.

Mathematics Subject Classification (2020): 26A33, 35R11, 42C40, 65M70

1. Introduction

Fractional calculus expands traditional calculus to encompass non-integer orders. The fact that fractional integrals and derivatives are quasi-differential operators gives them the ability to possess

Email addresses: chshahid9092@gmail.com (Shahid Ahmad), bhartiyadav4170@gmail.com (Bharti Yadav), pooja.vats@krmangalam.edu.in (Pooja Vats), rakshakmc@gmail.com (Raksha Sharma)*

Received February 17, 2025; Accepted March 29, 2025; Online 22 April, 2025

nonlocal features. As a result, they serve as useful instruments for characterising the memory and genetic features of many materials and processes. These operators are typically used to generalise differential equations, allowing for more flexibility in modelling various physical phenomena or mathematical problems. Dynamic processes in complex systems are regulated by anomalous diffusion [1, 2]. Fractional calculus has a long and illustrious history that has been distinguished through rapid progress and extensive application across various fields [1, 2, 3, 4]. It finds relevance in modeling nonlinear oscillations in hydrodynamic systems [7], colored noise analysis [9], earthquakes [6], physical phenomena , solid mechanics [10], economics [11], anomalous transport phenomena [13], bioengineering [12] continuous statistical mechanics [8],, and numerous other domains. Fractional partial differential equations (FPDEs) employ noninteger-order derivatives, enabling effective representation of memory and genetic properties within matter. The concept of fractional derivatives is significant in a wide variety of fields, including fluid mechanics, mathematical biology, engineering, physics, and as many other fields as possible. When viewed in a fractional perspective, the fractional convection-diffusion equation (FCDE) appears as a significant model for the simulation of various anomulus diffusion processes. By including fractional-order time derivatives, this equation enhances the conventional convection-diffusion model, which in turn provides a more realistic representation of complex temporal dynamics. These equations are essential for modelling anomalous diffusion processes, which exhibit non-standard behaviours, especially in heterogeneous or disordered media. They are particularly important for modelling. For the purpose of this paper, we will concentrate on FCDEs that have variable coefficients as follows:

$$\frac{\partial^{\alpha} x(\rho,\theta)}{\partial \theta^{\alpha}} + r(\rho)\frac{\partial x(\rho,\theta)}{\partial \rho} + p(\rho)\frac{\partial^{2} x(\rho,\theta)}{\partial \rho^{2}} = h(\rho,\theta), \quad 0 < \rho < 1, 0 < \theta \leq 1 \tag{1}$$

with initial and boundary conditions

$$x(\rho,0) = f(\rho), \tag{2}$$

$$x(0,\theta) = h_0(\theta), \quad x(1,\theta) = h_1(\theta), \tag{3}$$

where $0 < \alpha < 1$ and $r(\rho)$, $p(\rho) \neq 0$ are continuous function $f(.), h_0(.), h_1(\cdot)$ are function in $L^2[0,1)$ and $h(.,.)$ is a given function in $L^2([0,1) \times [0,1))$. For the purpose of defining the time fractional derivative, the Caputo fractional derivatives are used in this particular circumstance.

Practical applications such as modelling oil reservoirs, analysing mass and energy movement, and studying dispersion in chemical reactors may benefit from the fractional derivative in time because it provides a more detailed portrayal of memory effects and long-range interactions. When confronted with situations displaying anomalous diffusion features, where conventional differential equations may not be enough, this improved modelling capacity becomes very useful. Using the time-fractional convection-diffusion equation in simulations allows scientists and engineers to better understand how systems controlled by non-local temporal interactions behave. Many researchers have attempted to solve the aforementioned equation using various methods. For instance, the Chebyshev wavelet collocation method was proposed in [14]. Another approach by radial basis function method with a modified finite integration method [15]. The sinc-Galerkin method was introduced in [16], while the Sinc-Legendre collocation method was proposed in [16]. Additionally, the Chebyshev collocation method was developed in a separate study [17]. When the equation involves constant coefficients, a collocation method based on RBF was developed [18]. Finite difference and finite element methods were used to solve FCDEs [19, 20]. The numerical approaches that are based on wavelets provide a powerful alternative to the techniques that are already in use. Wavelet-based numerical approaches are used for solving FCDEs because they provide multi-resolution analysis, allowing for effective treatment of both global trends and local details. Their adaptive mesh refinement focuses computing resources on areas with steep gradients, increasing accuracy without incurring major computational

costs. Wavelets' localised character successfully deals with singularities and irregularities, and its sparse representation saves the computation cost. Furthermore, wavelet algorithms excel in computing fractional derivatives and managing variable coefficients, with high-order accuracy and convergence rates. These benefits make wavelet-based approaches especially resilient and efficient for the complicated nature of FCDEs. Different types of wavelet based methods have been used to solved fractional order integral and differential equations such as Haar wavelets [27], Euler wavelets [25], Fibonacci wavelets [13], Legendre wavelets [24], Laguerre wavelets [24], harmonic wavelets [22] and Gegenbour wavelets [23], are only a few of wavelet families that may be used to many physical, technical, and biological problems.

Among the wavelet families, the Bell wavelet is a more recent addition. However, they have already garnered considerable interest from researchers in numerous pure and applied mathematics disciplines. Combinatorial applications of bell polynomials have extended to theoretical physics, stochastic processes, and differential equations. In [28] Bell wavelet methods have been used to solve fractional integrodifferential equations and Bell polynomials are used to find superposition wave solutions of Hirota–Satsuma coupled KdV equations [29]. The Bell collocation method, utilizing Bell polynomials, has been developed to solve various mathematical problems, including linear integro-differential equations [34], fractional differential equations [35], and Fredholm integro-differential equations with variable coefficients. Additionally, the operational matrix method, based on Bell polynomials, has been extended to solve Fredholm-Volterra integro-differential equations [37]. Taylor operational method for the solutions of pantograph equations [38], and the operational matrix method for solving the Lotka-Volterra predator-prey model with discrete delays [39]. In this study, we developed a new approach for solving FCDEs by developing operational matrices based on Bell wavelet. This method transforms FCDEs into an algebraic system of equations. The accuracy and effectiveness of the approach that we have presented have been validated by numerical examples. The structure of this work is as follows: Following a survey of the existing research on time FCDEs and their solutions, Section 2 provides an overview of Bell polynomials and a fundamental introduction to fractional derivatives. In Section 3, Bell wavelet and operational matrix of integration of Bell wavelets are discussed and also the function approximations. In section 4, Fractional OMI of Bell wavelet is presented. In section 5 the method of description of proposed technique is given. In Section 6, In addition to numerical illustrations, convergence and error analysis are also covered. Lastly, a brief conclusion was drawn in section 7.

2. Preliminaries

Here, we provide definitions related to fractional calculus, Bell polynomials

Fractional calculus

Definition 2.1: *For any function* $y(\theta) \in C_{\omega}$ *with* $\omega \geq -1$*, the Riemann-Liouville (R-L) fractional integration operator* I^{α} *(for* $\alpha > 0$*) is defined as:*

$$I^{\alpha} y(\theta) = \begin{cases} y(\theta), & \theta = 0, \\ \dfrac{1}{\Gamma(\alpha)} \displaystyle\int_0^{\theta} (\theta - x)^{\alpha - 1} \theta(x) dx, & \alpha > 0. \end{cases} \tag{4}$$

The properties of the R-L fractional integration operator I^{α} for $\alpha, \beta > 0$ include:

- $I^{\alpha} I^{\beta} y(\theta) = I^{\beta} I^{\alpha} y(\theta)$,
- $I^{\alpha} I^{\beta} y(\theta) = I^{\alpha+\beta} y(\theta)$,
- $I^{\alpha} \theta^{\upsilon} = \dfrac{\Gamma(1+\upsilon)}{\Gamma(1+\alpha+\upsilon)} \theta^{\alpha+\upsilon}, \quad \upsilon > -1.$

Definition 2.2: *For any function* $y(\theta) \in C_{-1}^{n}$, *the Liouville-Caputo fractional derivative operator* $\mathcal{D}^{\alpha}$ *is defined as follows:*

$$D^{\alpha} y(\theta) = \begin{cases} \theta^{(n)}(\theta), & \alpha = n \in \mathbb{N}, \\ \dfrac{1}{\Gamma(n-\alpha)} \displaystyle\int_0^{\theta} \frac{\theta^{(n)}(x)}{(\theta - x)^{\alpha+1-n}} dx, & n-1 < \alpha < n, n \in \mathbb{N}. \end{cases} \tag{5}$$

From (4) and (5), we get

- $D^{\alpha} I^{\alpha} y(\theta) = y(\theta)$,
- $D^{\beta} I^{\alpha} y(\theta) = I^{\alpha-\beta} y(\theta), \quad \alpha > \beta$,
- $I^{\alpha} D^{\beta} y(\theta) = y(\theta) - \sum_{k=0}^{n-1} \theta^{k} \left(0^{+}\right) \dfrac{\theta^{k}}{k!}, \quad \theta > 0, \quad n-1 < \alpha \le n$.

Bell polynomial

Bell polynomials $\mathbb{B}_n(\theta)$ of order n, are defined by [28]

$$\mathbb{B}_n(\theta) = \sum_{k=0}^{n} S(n,k) \theta^{k},$$

here $S(n,k)$ represents the second kind Stirling number and define as:

$$S(n,k) = \sum_{i=0}^{k} \frac{(-1)^{i}}{k!} \binom{k}{i} (k-i)^{n}.$$

Utilizing the characteristics of Bell polynomials, the vector $\mathbb{B}(\theta) = \left[\mathbb{B}_0(\theta), \cdots, \mathbb{B}_n(\theta)\right]$, which comprise the Bell polynomials $\mathbb{B}_j(\theta)$ for $j = 0,1,\cdots,n$, is expressed as:

$$\mathbb{B}(\theta) = \mathbf{S}\mathbf{Y}(\theta), \tag{6}$$

where

$$\mathbf{Y}(\theta) = \left[1, \theta, \cdots, \theta^{n}\right]^{T}$$

and

$$\mathbf{S} = \begin{bmatrix} S(0,0) & 0 & \cdots & 0 \\ S(1,0) & S(1,1) & \cdots & 0 \\ \vdots & \vdots & \ddots & \vdots \\ S(n,0) & S(n,1) & \cdots & S(n,n) \end{bmatrix}$$

Since the matrix $\mathbf{S}$ is nonsingular and lower triangular with nonzero diagonal elements, its inverse $\mathbf{S}^{-1}$ exists. Consequently, equation (6) can be rewritten as:

$$Y(\theta) = \mathbf{S}^{-1} \mathbb{B}(\theta).$$

Starting Bell polynomials are

$$\begin{aligned}
&\mathbb{B}_0(\theta) = 1,\\
&\mathbb{B}_1(\theta) = \theta,\\
&\mathbb{B}_2(\theta) = \theta^2 + \theta,\\
&\mathbb{B}_3(\theta) = \theta^3 + 3\theta^2 + \theta,\\
&\mathbb{B}_4(\theta) = \theta^4 + 6\theta^3 + 7\theta^2 + \theta,\\
&\mathbb{B}_5(\theta) = \theta^5 + 10\theta^4 + 25\theta^3 + 15\theta^2 + \theta,\\
&\mathbb{B}_6(\theta) = \theta^6 + 15\theta^5 + 65\theta^4 + 90\theta^3 + 31\theta^2 + \theta.
\end{aligned}$$

3. Bell Wavelet and Operational Matrices of Integration

The Bell wavelets $\psi_{mn}(\theta) = \psi(k,m,n,\theta)$ have four arguments: $k \in \mathbb{Z}^+$, $m = 1,\ldots,2^{k-1}$, the θ is the normalized time and degree of the Bell polynomials is given by n. On the interval [0,1), Bell wavelets are given by

$$\psi_{mn}(\theta) = \begin{cases} 2^{\frac{k-1}{2}}\,\mathbb{B}_{\mathrm{n}}\left(2^{k-1}\theta - m + 1\right), & \dfrac{m-1}{2^{k-1}} \le \theta < \dfrac{m}{2^{k-1}},\\ 0, \quad \text{otherwise.} \end{cases} \tag{7}$$

The Bell wavelets basis for k=2, M=3 are

$$\psi_{1,0}(\theta) = \begin{cases} \sqrt{2}, & 0 \le \theta < \dfrac{1}{2},\\ 0, & \text{otherwise.} \end{cases}$$

$$\psi_{1,1}(\theta) = \begin{cases} 2\sqrt{2}\theta, & 0 \le \theta < \dfrac{1}{2},\\ 0, & \text{otherwise.} \end{cases}$$

$$\psi_{1,2}(\theta) = \begin{cases} 4\sqrt{2}\theta^2 + 2\sqrt{2}\theta, & 0 \le \theta < \dfrac{1}{2},\\ 0, & \text{otherwise.} \end{cases}$$

$$\psi_{2,0}(\theta) = \begin{cases} \sqrt{2}, & \dfrac{1}{2} \le \theta < 1,\\ 0, & \text{otherwise.} \end{cases}$$

$$\psi_{2,1}(\theta) = \begin{cases} 2\sqrt{2}\theta - \sqrt{2}, & \dfrac{1}{2} \le \theta < 1,\\ 0, & \text{otherwise.} \end{cases}$$

$$\psi_{2,2}(\theta) = \begin{cases} 4\sqrt{2}\theta^2 - 2\sqrt{2}\theta, & \dfrac{1}{2} \le \theta < 1,\\ 0, & \text{otherwise.} \end{cases}$$

The matrix will be for k=2, M=3

$$\psi_{6\times 6}=\begin{bmatrix} 1.4142 & 1.4142 & 1.4142 & 0 & 0 & 0 \\ 0.2357 & 0.7071 & 1.1785 & 0 & 0 & 0 \\ 0.2750 & 1.0607 & 2.1606 & 0 & 0 & 0 \\ 0 & 0 & 0 & 1.4142 & 1.4142 & 1.4142 \\ 0 & 0 & 0 & 0.2357 & 0.7071 & 1.1785 \\ 0 & 0 & 0 & 0.2750 & 1.0607 & 2.1606 \end{bmatrix}.$$

The integrals that will be used to solve fractional telegraph equations are as follows:

$$q_{m,n}(\theta)=\int_0^\theta \psi_{mn}(z)dz, \quad p_{m,n}(\theta)=\int_0^\theta p_{mn}(z)dz \tag{8}$$

and the elements of the matrices for (8) are given by

$$(q_{m,n})_{2^{k-1}\times M}=\begin{pmatrix} q_{1,0}(\theta) & q_{1,1}(\theta) & \cdots & q_{1,M-1}(\theta) \\ q_{2,0}(\theta) & q_{2,1}(\theta) & \cdots & q_{2,M-1}(\theta) \\ \vdots & \vdots & \ddots & \vdots \\ q_{2^{k-1},0} & q_{2^{k-1},1} & \cdots & q_{2^{k-1},M-1}(\theta) \end{pmatrix}_{2^{k-1}\times M}$$

and

$$(p_{m,n})_{2^{k-1}\times M}=\begin{pmatrix} p_{1,0}(\theta) & p_{1,1}(\theta) & \cdots & p_{1,M-1}(\theta) \\ p_{2,0}(\theta) & p_{2,1}(\theta) & \cdots & p_{2,M-1}(\theta) \\ \vdots & \vdots & \ddots & \vdots \\ p_{2^{k-1},0} & p_{2^{k-1},1} & \cdots & p_{2^{k-1},M-1}(\theta) \end{pmatrix}_{2^{k-1}\times M}$$

By taking k=2, M=3

$$q_{1,0}(\theta)=\begin{cases} \sqrt{2}\theta, & 0\le\theta<\dfrac{1}{2}, \\ \dfrac{\sqrt{2}}{2}, & \dfrac{1}{2}\le\theta<1. \end{cases}$$

$$q_{1,1}(\theta)=\begin{cases} \sqrt{2}\theta^2, & 0\le\theta<\dfrac{1}{2}, \\ \dfrac{\sqrt{2}}{4}, & \dfrac{1}{2}\le\theta<1. \end{cases}$$

$$q_{1,2}(\theta)=\begin{cases} 2\sqrt{2}\left(\dfrac{2}{3}\theta^3+\dfrac{\theta^2}{2}\right), & 0\le\theta<\dfrac{1}{2}, \\ 2\sqrt{2}\left(\dfrac{5}{24}\right), & \dfrac{1}{2}\le\theta<1. \end{cases}$$

$$q_{2,0}(\theta)=\begin{cases} \sqrt{2}\left(\theta-\dfrac{1}{2}\right), & \dfrac{1}{2}\le\theta<1, \\ 0, & \text{otherwise.} \end{cases}$$

$$q_{2,1}(\theta)=\begin{cases}\sqrt{2}\left(\theta^2-\theta+\frac{1}{4}\right), & \frac{1}{2}\le\theta<1,\\ 0, & \text{otherwise.}\end{cases}$$

$$q_{2,2}(\theta)=\begin{cases}2\sqrt{2}\left(\frac{2}{3}\theta^2-\frac{\theta^2}{2}-\frac{5}{24}\right), & \frac{1}{2}\le\theta<1.,\\ 0, & \text{otherwise.}\end{cases}$$

and

$$p_{1,0}(\theta)=\begin{cases}\frac{1}{\sqrt{2}}\theta^2, & 0\le\theta<\frac{1}{2},\\ \sqrt{2}\left(\frac{\theta}{2}-\frac{1}{8}\right), & \frac{1}{2}\le\theta<1.\end{cases}$$

$$p_{1,1}(\theta)=\begin{cases}\frac{\sqrt{2}}{3}\theta^3, & 0\le\theta<\frac{1}{2},\\ \sqrt{2}\left(\frac{\theta}{4}-\frac{1}{12}\right), & \frac{1}{2}\le\theta<1.\end{cases}$$

$$p_{1,2}(\theta)=\begin{cases}2\sqrt{2}\left(\frac{1}{6}\theta^4+\frac{\theta^3}{6}\right), & 0\le\theta<\frac{1}{2},\\ 2\sqrt{2}\left(\frac{5}{24}\theta-\frac{7}{96}\right), & \frac{1}{2}\le\theta<1.\end{cases}$$

$$p_{2,0}(\theta)=\begin{cases}\sqrt{2}\left(\frac{\theta^2}{2}-\frac{\theta}{2}+\frac{1}{8}\right), & \frac{1}{2}\le\theta<1,\\ 0, & \text{otherwise.}\end{cases}$$

$$p_{2,1}(\theta)=\begin{cases}\sqrt{2}\left(\frac{\theta^3}{3}-\frac{\theta^2}{2}+\frac{\theta}{4}-\frac{1}{24}\right), & \frac{1}{2}\le\theta<1,\\ 0, & \text{otherwise.}\end{cases}$$

$$p_{2,2}(\theta)=\begin{cases}2\sqrt{2}\left(\frac{1}{6}\theta^4-\frac{\theta^3}{6}-\frac{5}{24}\theta-\frac{9}{96}\right), & \frac{1}{2}\le\theta<1,\\ 0, & \text{otherwise.}\end{cases}$$

3.1. Function Approximations

A function $x(\theta)\in L^2[0,1]$ could be represented in form of Bell wavelets as:

$$x(\theta)=\sum_{m=0}^{\infty}\sum_{n\in Z^+}c_{mn}\psi_{mn}(\theta).$$

By truncating above equation, we get

$$x(\theta) \simeq \sum_{m=1}^{2^{k-1}} \sum_{n=0}^{M-1} c_{mn} \psi_{mn}(\theta), \tag{9}$$

where

$$c_{\mathrm{m,n}} = \int_0^1 x(\theta) \psi_{\mathrm{m,n}}(\theta) d\theta,$$

are the coefficients of Bell wavelet. The equation (9) can be expressed as a matrix:

$$x(\theta) = C^T \Psi(\theta), \tag{10}$$

here we define the row vector C as:

$$C = \left[c_{1,0}, \ldots, c_{1,M-2}, c_{1,M-1}, c_{2,0}, \cdots, c_{2,M-2}, c_{2,M-1}, \ldots, c_{2^{k-1},0}, c_{2^{k-1},1}, \ldots, c_{2^{k-1},M-1} \right]^T. \tag{11}$$

The matrix $\Psi(\theta)$ in (10) is $1 \times 2^{k-1} M$ order Bell wavelet matrix is as

$$\Psi(\theta) = \left[\psi_{1,0}, \cdots, \psi_{1,M-2}, \psi_{1,M-1}, \psi_{2,0}, \ldots, \psi_{2,M-2}, , \psi_{2,M-1}, \ldots, \psi_{2^{k-1},0}, \psi_{2^{k-1},1}, \ldots, \psi_{2^{k-1},M-1} \right]^T. \tag{12}$$

Finally, taking the collocation points:

$$\phi_\ell = \frac{2\ell - 1}{2^k M}, \quad \ell = 1, 2, \ldots, 2^{k-1} M. \tag{13}$$

From (7), the Bell wavelets in two dimension can be defined as:

$$\begin{aligned} &\psi_{\mathrm{m}_1,\mathrm{n}_1,\mathrm{m}_2,\mathrm{n}_2}(\theta,\delta) \\ &= \begin{cases} 2^{(k_1-1)/2} 2^{(k_2-1)/2} \mathbb{B}_{\mathrm{n}_1}\left(2^{k_1-1}\theta - \mathrm{m}_1 + 1\right) \mathbb{B}_{\mathrm{n}_2}\left(2^{k_2-1} t - \mathrm{m}_2 + 1\right), \\ \qquad \dfrac{\mathrm{m}_1 - 1}{2^{k_1-1}} \le \theta < \dfrac{\mathrm{m}_1}{2^{k_1-1}}, \dfrac{\mathrm{m}_2 - 1}{2^{k_2-1}} \le \delta < \dfrac{\mathrm{m}_2}{2^{k_2-1}} \\ \qquad\qquad 0, \quad \text{otherwise}, \end{cases} \end{aligned} \tag{14}$$

where $\mathrm{m}_1, \mathrm{n}_1, \mathrm{m}_2, \mathrm{n}_2, k_1$ and k_2 have the usual meanings and $\psi_{\mathrm{m}_1,\mathrm{n}_1,\mathrm{m}_2,\mathrm{n}_2}(\theta,\delta)$ constitutes a basis for $L^2([0,1) \times [0,1))$.

So, equation (14) can be expressed by any arbitrary function $x(\theta,\delta) \in L^2([0,1) \times [0,1))$ as

$$\begin{aligned} x(\theta,\delta) &= \sum_{\mathrm{m}_1=1}^{2^{k_1-1}} \sum_{\mathrm{n}_1=0}^{M_1-1} \sum_{\mathrm{m}_2=1}^{2^{k_2-1}} \sum_{\mathrm{n}_2=0}^{M_2-1} c_{\mathrm{m}_1,\mathrm{n}_1,\mathrm{m}_2,\mathrm{n}_2} \psi_{\mathrm{m}_1,\mathrm{n}_1}(\theta) \psi_{\mathrm{m}_2,\mathrm{n}_2}(\delta) \\ &= \psi^T(\theta) \mathrm{C} \psi(\delta), \end{aligned} \tag{15}$$

here, C is the matrix of order $2^{k_1-1} M_1 \times 2^{k_2-1} M_2$ composed of Bell wavelet coefficients

$$\begin{aligned} c_{\mathrm{m}_1,\mathrm{n}_1,\mathrm{m}_2,\mathrm{n}_2} = \; & \int_0^1 \int_0^1 x(\theta,\delta) \psi_{\mathrm{m}_1,\mathrm{n}_1}(\theta) \psi_{\mathrm{m}_2,\mathrm{n}_2}(\delta) d\theta d\delta, \\ & 1 \le \mathrm{m}_1 \le 2^{k_1-1}, 0 \le \mathrm{n}_1 \le M_1 - 1, \\ & 1 \le \mathrm{m}_2 \le 2^{k_2-1}, 0 \le \mathrm{n}_2 \le M_2 - 1. \end{aligned} \tag{16}$$

Finally, taking collocation point:

$$\begin{aligned}\phi_{\ell_1} &= \frac{2\ell_1 - 1}{2^{k_1} M_1}, \quad \ell_1 = 1,2,\ldots,2^{k_1-1} M_1.\\ \phi_{\ell_2} &= \frac{2\ell_2 - 1}{2^{k_2} M_2}, \quad \ell_2 = 1,2,\ldots,2^{k_2-1} M_2.\end{aligned} \tag{17}$$

4. Fractional OMI of Bell Wavelet

On $[0,1)$ interval, the BPFs are given by

$$\mathrm{b}_\nu(\theta) = \begin{cases} 1 & \nu q \le \theta < (\nu+1)q, \\ 0 & \text{otherwise.} \end{cases} \tag{18}$$

where $q = \frac{1}{N}$ and for $N \in \mathbb{Z}^+$, $\nu = 0,1,\ldots,N-1$.

The function $y(\theta) \in L^2[0,1)$ estimated via of BPFs.

$$y(\theta) \simeq y_N(\theta) = \sum_{\nu=1}^{N-1} b_\nu g_\nu(\theta) = B^T G_N, \tag{19}$$

where $G_N = [G_0, G_1, G_2, ..., G_N]^T$ and $B = [b_0, b_1, b_2, ..., b_N - 1]$. Integrating the vector $G_N(\theta)$, we get

$$\int_0^\theta G_N(y)dy \simeq \Delta G_N(\theta), \tag{20}$$

so the OMI for BPFs is defined as follow:

$$\Delta = \frac{q}{2}\begin{pmatrix} 1 & 2 & 2 & \ldots & 2 \\ 0 & 1 & 2 & \ldots & 2 \\ \vdots & \vdots & \vdots & \cdots & \vdots \\ 0 & 0 & 0 & \cdots & 1 \end{pmatrix} \tag{21}$$

Then, by using BPFs to describes the OMI of fractional order H^α as

$$\left(I^\alpha G_N\right)(\theta) \simeq H^\alpha G_N(\theta), \tag{22}$$

where

$$H^\alpha = \frac{1}{N^\alpha \Gamma(\alpha+2)}\begin{pmatrix} 1 & \theta_1 & \theta_2 & \theta_3 & \ldots & \theta_{N-1} \\ 0 & 1 & \theta_1 & \theta_2 & \ldots & \theta_{N-2} \\ 0 & 0 & 1 & \theta_1 & \ldots & \theta_{N-3} \\ \vdots & \vdots & \vdots & \vdots & \ldots & \vdots \\ 0 & 0 & \ldots & 0 & 1 & \theta_1 \\ 0 & 0 & 0 & \ldots & 0 & 1 \end{pmatrix}, \tag{23}$$

where, the θ_ν 's in (23) have been defined as:

$$\theta_\nu = (\nu+1)^{\alpha+1} - 2\nu^{\alpha+1} + (\nu-1)^{\alpha+1}. \tag{24}$$

4.1. OMI of Bell Wavelet

Here, we utilize Block Pulse Functions (BPFs) to construct fractional order integration matrices associated with Bell wavelets by performing integration on equation (12) as:

$$\int_0^\theta \Psi(y)dy \approx O\Psi(\theta), \tag{25}$$

where O represents the OMI for $2^{k-1}M \times 2^{k-1}M$ order of Bell wavelet. It is worth mentioning that BPFs (18) are used to represent the Bell wavelets (12) as

$$\psi(\theta) = \psi_{\mathrm{m,n}} G_N(\theta) \tag{26}$$

To get the OMI for order α of Bell wavelet, we define

$$I^\alpha \psi(\theta) = O^\alpha_{\mathrm{m,n}} \psi(\theta), \tag{27}$$

where the $O^\alpha_{\mathrm{m,n}}$ matrix define the Bell wavelet's OMI of fractional order, by taking the relationships (22), (26) and (27) we get

$$\left(I^\alpha \psi\right)(\theta) \approx \left(I^\alpha \psi_{\mathrm{m,n}} G_N\right)(\theta) = \psi_{\mathrm{m,n}} \left(I^\alpha G_N\right)(\theta) \approx \psi_{\mathrm{m,n}} H^\alpha G_N(\theta). \tag{28}$$

Since, from (27) and (28), we obtain:

$$O^\alpha_{\mathrm{m,n}} \psi(\theta) = O^\alpha_{\mathrm{m,n}} \psi_{\mathrm{m,n}} G_N(\theta) = \psi_{\mathrm{m,n}} H^\alpha G_N(\theta), \tag{29}$$

which yields in the necessary OMI of general order for the Bell wavelets:

$$O^\alpha_{\mathrm{m,n}} = \psi_{\mathrm{m,n}} H^\alpha \left[\psi_{\mathrm{m,n}}\right]^{-1}. \tag{30}$$

For instance, at $\alpha = 0.6,\ k = 2, M = 3$, the corresponding fractional OMI $O^{0.6}_{6\times 6}$ corresponding with the Bell wavelets is given by:

$$O^{0.6}_{6\times 6} = \begin{pmatrix} 0.0892 & 1.2664 & -0.3166 & 0.6498 & -0.7848 & 0.2653 \\ 0.0059 & -0.1658 & 0.3166 & 0.3712 & -0.5411 & 0.1895 \\ 0.0222 & -0.7797 & 0.7927 & 0.6306 & -0.9550 & 0.3368 \\ 0 & 0 & 0 & 0.0892 & 1.2664 & -0.3166 \\ 0 & 0 & 0 & 0.0059 & -0.1658 & 0.3166 \\ 0 & 0 & 0 & 0.0222 & -0.7797 & 0.7927 \end{pmatrix}. \tag{31}$$

5. Description of Method

This section aims to illustrate how OMI can be applied to construct solutions using Bell wavelets to solve FCDEs having initial and boundary conditions

Let us take FCDEs with variable coefficient and $0 < \rho < 1, \quad 0 < \theta \le 1, \quad 0 < \alpha < 1$

$$\frac{\partial^\alpha x(\rho,\theta)}{\partial \theta^\alpha} + r(\rho)\frac{\partial x(\rho,\theta)}{\partial \rho} + p(\rho)\frac{\partial^2 x(\rho,\theta)}{\partial \rho^2} = h(\rho,\theta) \tag{32}$$

with initial condition

$$x(\rho,0) = f(\rho), \quad 0 < \rho < 1, \tag{33}$$

and boundary conditions

$$\begin{aligned} x(0,\theta) &= h_0(\theta), \\ x(1,\theta) &= h_1(\theta). \end{aligned} \tag{34}$$

To solve equation (32) assume that

$$\frac{\partial^{2+\alpha} x(\rho,\theta)}{\partial\rho^2\partial\theta^\alpha} \approx \Psi^{\mathrm{T}}(\rho) G \Psi(\theta) \tag{35}$$

Incorporating an unknown Bell wavelet coefficient G, we utilize the R-L fractional integral of order α to integrate (35) w.r.t θ, then:

$$\frac{\partial^2 x(\rho,\theta)}{\partial\rho^2} \approx \left.\frac{\partial^2 x(\rho,\theta)}{\partial\rho^2}\right|_{\theta=0} + \Psi^{\mathrm{T}}(\rho) G\left(U^\alpha \Psi(\theta)\right) \tag{36}$$

where $U^\alpha = U^\alpha_{2^{k-1}M\times 2^{k-1}M}$ Using initial condition (33), enable to put in (36)

$$\frac{\partial^2 x(\rho,\theta)}{\partial\rho^2} \approx f''(\rho) + \Psi^{\mathrm{T}}(\rho) G U^\alpha \Psi(\theta) \tag{37}$$

By integrating (37) two times w.r.t ρ, we obtain

$$x(\rho,\theta) \approx x(0,\theta) + \rho \left.\frac{\partial x(\rho,\theta)}{\partial\rho}\right|_{\rho=0} + f(\rho) - f(0) - \rho f'(0) + \left(U^2\Psi(\rho)\right)^{\mathrm{T}} G\left(U^\alpha\Psi(\theta)\right) \tag{38}$$

Taking $\rho = 1$ in (38) and employing the conditions given in (34), we have

$$x(1,t) \approx x(0,\theta) + \left.\frac{\partial x\left(\rho,\theta\right)}{\partial\rho}\right|_{\rho=0} - f'(0) + f(0) - f(1) + \left(U^2\Psi(1)\right)^{\mathrm{T}} G\left(U^\alpha\Psi(\theta)\right) \tag{39}$$

So, it become

$$\left.\frac{\partial x(\rho,\theta)}{\partial\rho}\right|_{\rho=0} \approx -\left(U^2\Psi(1)\right)^{\mathrm{T}} G\left(U^\alpha\Psi(\theta)\right) + f(0) + f'(0) - f(1) + h_1(\theta) - h_1(\theta) = R(\theta) \tag{40}$$

Substitute (40) in (38), we obtain

$$x(\rho,\theta) \approx \quad x(0,\theta) + \rho R(\theta) + f(\rho) - f(0) - \rho f'(0) + \left(U^2\Psi(\rho)\right)^{\mathrm{T}} G\left(U^\alpha\Psi(\theta)\right) \tag{41}$$

Differentiating equation (41) w.r.t ρ the following equation obtained,

$$\frac{\partial x(\rho,\theta)}{\partial\rho} \approx R(\theta) + f'(\rho) - f'(0) + (U\Psi(\rho))^T G\left(U^\alpha\Psi(\theta)\right) \tag{42}$$

Utilizing Caputo fractional derivative with respect to θ to equation (41), the following equation is derived:

$$\begin{aligned} &\frac{\partial^\alpha x(\rho,\theta)}{\partial\theta^\alpha} \approx \left(U^2\Psi(\rho)\right)^{\mathrm{T}} G\Psi(\theta) + \rho D^\alpha R(\theta) + D^\alpha h_1(\theta) \\ \text{where} \quad &D^\alpha R(\theta) = -\left(U^2\Psi(1)\right)^{\mathrm{T}} G\Psi(\theta) + \frac{\partial^\alpha}{\partial\theta^\alpha} h_1(\theta) \\ &D^\alpha h_1(\theta) = (1-\rho)\frac{\partial^\alpha h_1(\theta)}{\partial\theta^\alpha} \end{aligned} \tag{43}$$

By inserting the equations(37),(42),(43) in (32) and applying the given collocation points (13).
By substituting ≈ with =, we obtain the following system of algebraic equations:

$$\begin{aligned}&\left(U^2\Psi(\rho)\right)^{\mathrm{T}} G\Psi(\theta)+\rho D^{\alpha}R(\theta)+D^{\alpha}h_1(\theta)+r(\rho)(R(\theta)+f^{'}(\rho)-f^{'}(0)\\&+(U\Psi(\rho))^{T}G\left(U^{\alpha}\Psi(\theta)\right)+p(\rho)(f^{''}(\rho)+\Psi^{\mathrm{T}}(\rho)GU^{\alpha}\Psi(\theta))=h(\rho,\theta)\end{aligned}\tag{44}$$

We determine the unknown Bell coefficient G in (44) by solving the system using Newton iterative approach. Subsequently, by substituting G into (41), we derive an approximate solution to (32).

6. Numerical Simulation and Error Analysis

Here, we solve and compare four distinct problems to demonstrate the proposed technique's effectiveness and precision. The fundamental findings regarding the approximation of Bell polynomials serve as the foundation for exploring the convergence of Bell wavelets approximations as:

For any function $\varkappa(\lambda) \in L^2[0,1]$, and let $\mathcal{B}(\lambda)=\left[\mathbf{B}_0(\lambda),\mathbf{B}_1(\lambda)\cdots,\mathbf{B}_n(\lambda)\right]$ can be expressed as

$$\varkappa(\lambda)\approx\varkappa_n(\lambda)=\sum_{i=0}^{n}c_i\mathcal{B}(\lambda).\tag{45}$$

Lemma 6.1 provides an outline for proving the convergence of Bell polynomials.

Lemma 6.1 *[27] Consider $\varkappa(\lambda)\in L^2[0,1]$, where $\theta_n(\lambda)$ defined in (45), shows best approximation of the real function $\varkappa(\lambda)$ by the Bell polynomials. Therefore, ∃ a constant R as*

$$\left\|\varkappa(\lambda)-\varkappa_n(\lambda)\right\|_2\le\frac{R}{(n+1)!2^{2n+1}}.$$

here $R=\max_{\lambda\in[0,1]}\left|\varkappa^{n+1}(\lambda)\right|$.

Proof. One can see the proof in [27].

Remark 6.2: *From Lemma 6.1, if $n\to\infty$, then $\frac{1}{(n+1)!2^{2n+1}}\to 0$, which means $\varkappa_n(\lambda)\to\varkappa(\lambda)$.*

Theorem 6.3: *[26] Suppose the Bell wavelets expansion $\sum_{m=1}^{2^{k-1}}\sum_{n=0}^{M-1}c_{mn}\psi_{mn}(\lambda)=\sum_{j=0}^{\hat{m}}c_j\psi_j(\lambda)=C^{\mathrm{T}}\Psi(\lambda)$ of the smooth function $\varkappa(\lambda)$, therefore*

$$\lim_{\hat{m}\to\infty}\left\|\varkappa(\lambda)-\sum_{i=0}^{\hat{m}}c_i\psi_i(\lambda)\right\|=0,$$

where $\hat{m}=2^{k-1}M$.

Problem 6.4 *Consider the following FCDE as*

$$\frac{\partial^{\alpha}x(\rho,\theta)}{\partial\theta^{\alpha}}+\rho\frac{\partial x(\rho,\theta)}{\partial\rho}-\frac{\partial^2x(\rho,\theta)}{\partial\rho^2}=h(\rho,\theta)\tag{46}$$

$$0<\alpha<1,0<\rho<1,\quad 0<\theta\le 1.$$

with conditions as

$$\begin{aligned}x(\rho,0)&=\rho^2-\rho^3,\\x(0,\theta)&=x(1,\theta)=0,\end{aligned}\tag{47}$$

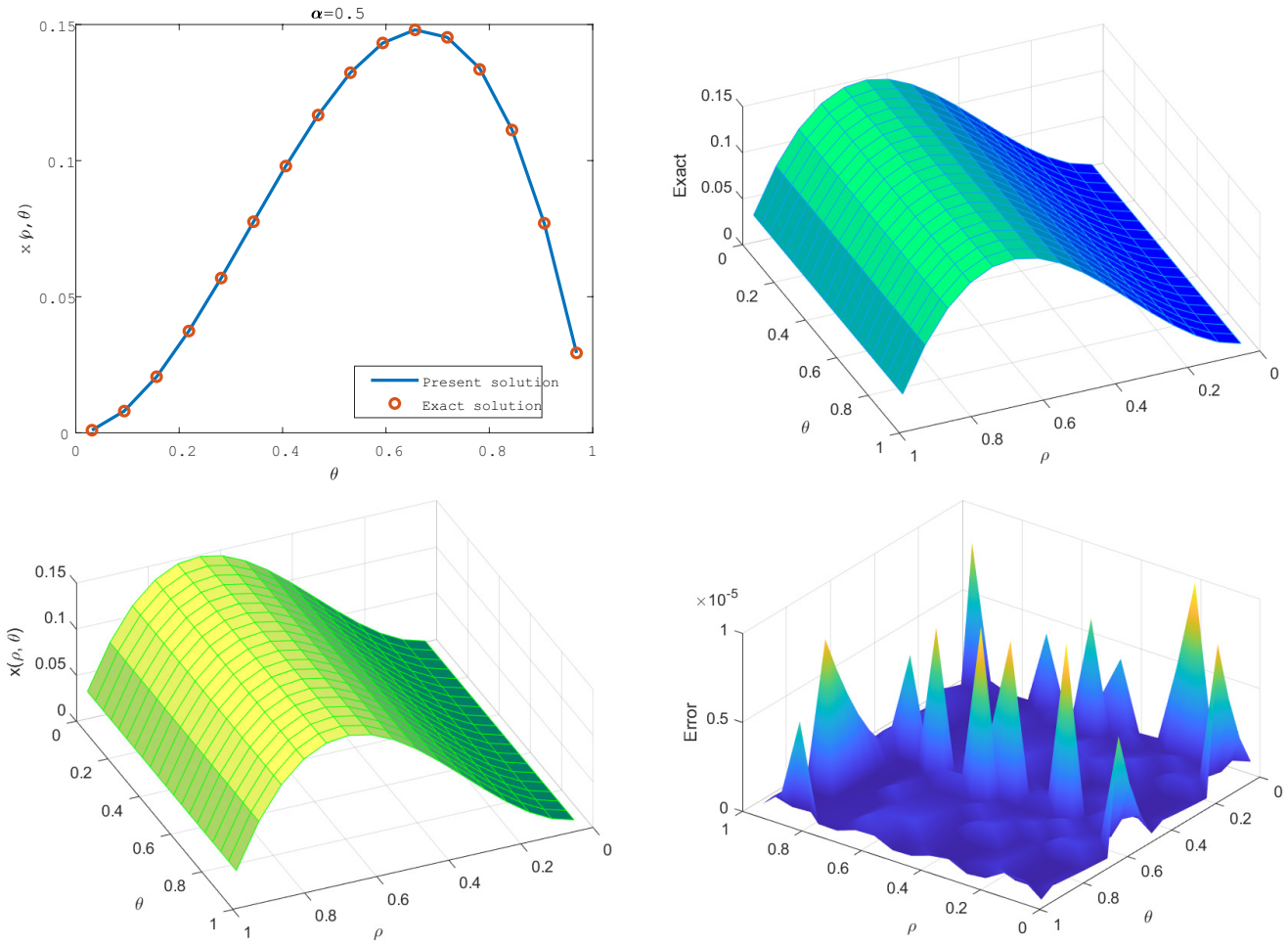

Figure 1: (A) 2D plot, (B,C) 3D Exact and approximate solutions respectively and (D) AE at $\alpha = 0.2$ of Problem 6.4.

where

$$h(\rho,\theta) = \frac{2\theta^{2-\alpha}}{\Gamma(3-\alpha)}\left(\rho^2 - \rho^3\right) + \left(\theta^2 + 1\right)\left(2\rho^2 - 3\rho^3 + 6\rho - 2\right) \tag{48}$$

The given problem has an exact solution provided below.

$$x(\rho,\theta) = \left(\theta^2 + 1\right)\left(\rho^2 - \rho^3\right). \tag{49}$$

In Figure 1A, we present a comparison between the solutions obtained using the Bell wavelet method and the exact solution for $\alpha = 0.5$ in two dimensions. The comparison is extended to three dimensions in Figures 1B,C, where the results clearly demonstrate the accuracy of the Bell wavelet approach. Additionally, Figure 1D graphically illustrates the absolute error, showcasing the method's precision. Furthermore, Table 1 provides a detailed comparison of the absolute error (AE) at different α against existing methods, highlighting the performance of our technique.

Problem 6.5:

Next, let us take the following TFCDE

$$\frac{\partial^\alpha x(\rho,\theta)}{\partial\theta^\alpha} + \rho\frac{\partial x(\rho,\theta)}{\partial\rho} + \frac{\partial^2 x(\rho,\theta)}{\partial\rho^2} = 2\theta^\alpha + 2\rho^2 + 2, \tag{50}$$

Table 1: AE of Problem 6.4 at different values of α and ρ, with truncated sample sizes: Fibonacci wavelet ($k=2, M=3$) and Present method ($k=2, M=3$)

ρ	Fibonacci wavelet [30]		Present method	
	α=0.7	α=0.5	α=0.7	α=0.5
.1	1.2085e-07	8.1341e-08	6.9595e-10	2.3851e-09
.2	7.6121e-07	1.7563e-07	4.0399e-09	1.3966e-09
.3	1.5390e-07	1.4571e-07	4.1779e-08	1.4507e-08
.4	3.4718e-06	8.6468e-07	9.7434e-08	3.4106e-08
.5	1.9165e-06	5.5723e-07	4.5805e-08	1.6554e-08
,6	1.0258e-07	1.2482e-07	3.0614e-08	1.0851e-08
.7	6.1842e-07	2.2037e-07	2.3966e-08	8.6611e-08
.8	6.5283e-07	2.2150e-07	4.0649e-09	1.5260e-08
.9	9.2498e-07	3.4541e-07	1.7608e-08	6.3425e-09

$$0<\alpha<1, \quad 0<\rho<1, \quad 0<\theta\leq 1.$$

with conditions as

$$\begin{aligned} &x(\rho,0)=\rho^2, 0<\rho<1,\\ &x(0,\theta)=\frac{2\Gamma(\alpha+1)}{\Gamma(2\alpha+1)}\theta^{2\alpha}, \quad x(1,\theta)=1+\frac{2\Gamma(\alpha+1)}{\Gamma(2\alpha+1)}\theta^{2\alpha}, 0\leq\theta\leq 1. \end{aligned} \tag{51}$$

Exact solution of (50) is

$$x(\rho,\theta)=\rho^2+\frac{2\Gamma(\alpha+1)}{\Gamma(2\alpha+1)}t^{2\alpha} \tag{52}$$

In Figure 2A, we present a comparison between the solutions obtained using the Bell wavelet method and the exact solution for $\alpha=0.5$ in two dimensions. The comparison is extended to three dimensions in Figures 2B,C, the outcomes conclusively demonstrate the precision of the Bell wavelet method. Additionally, Figure 2D graphically illustrates the absolute error, showcasing the method's precision. Furthermore, Table 2 provides a detailed comparison of the AE at different α against existing methods, highlighting the superior performance of our technique.

Problem 6.6: *Consider the following TFCDE (*$0<\alpha<1$*)*

$$\frac{\partial^\alpha x(\rho,\theta)}{\partial\theta^\alpha}+\rho\frac{\partial x(\rho,\theta)}{\partial\rho}-\frac{\partial^2 x(\rho,\theta)}{\partial\rho^2}=h(\rho,\theta), 0<\rho<1, 0<\theta\leqslant 1, \tag{53}$$

with conditions given below as:

$$\begin{aligned} &x(\rho,0)=\rho-\rho^3,\\ &x(0,\theta)=x(1,\theta)=0, \end{aligned} \tag{54}$$

where

$$h(\rho,\theta)=\frac{\Gamma(1+2\alpha)}{\Gamma(1+\alpha)}\theta^\alpha\left(\rho-\rho^3\right)+\left(1+\theta^{2\alpha}\right)\left(7\rho-3\rho^3\right). \tag{55}$$

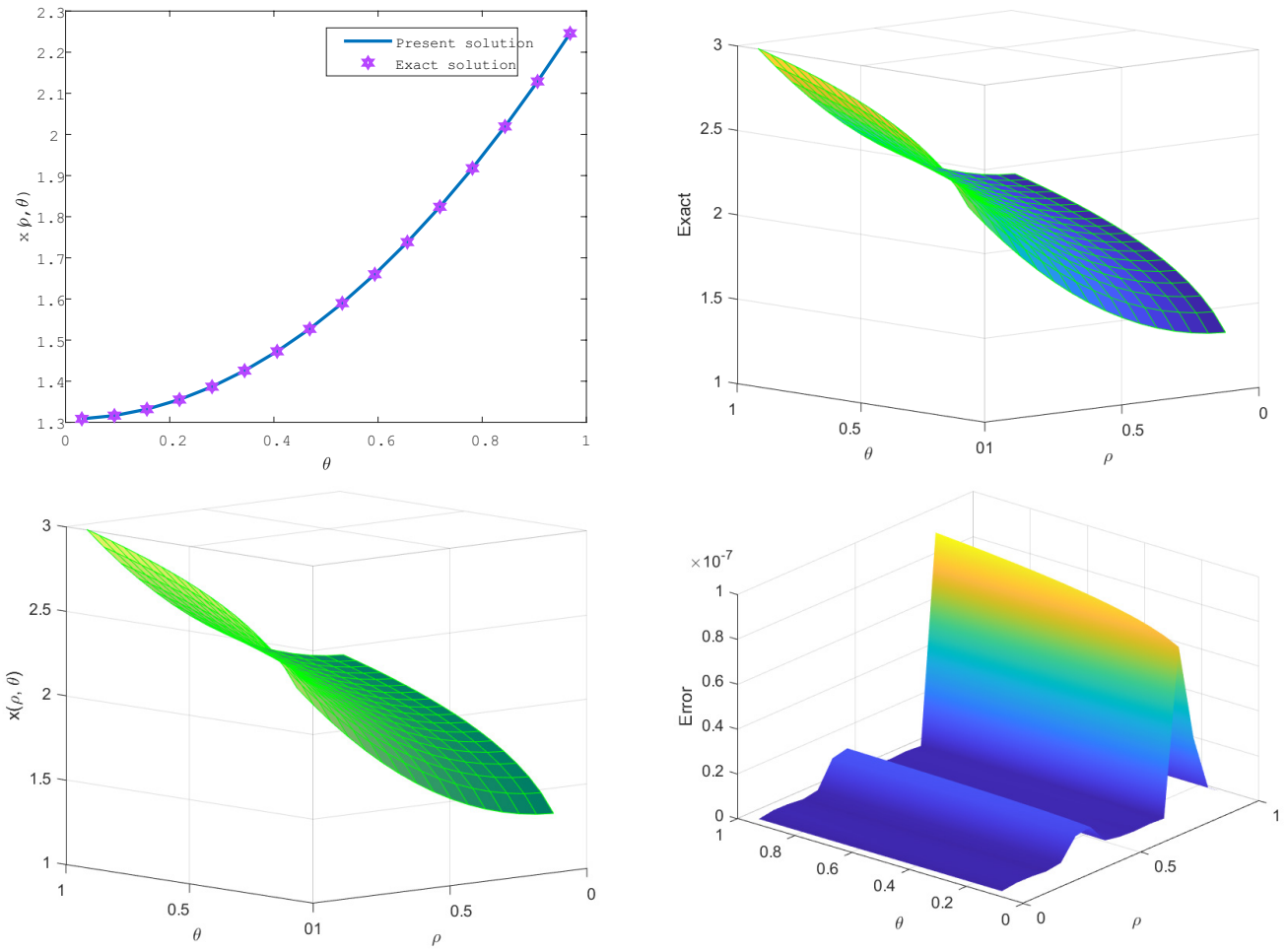

Figure 2: (A) 2D plot, (B,C) 3D Exact and approximate solutions respectively and (D) AE at $\alpha = 0.5$ of Problem 6.5.

Table 2: AE of Problem 6.5 at $\alpha = 0.5$, $\rho = 0.5$.

ρ	Present	Haar wavelet [3]		B-Spline Sinc [33]		Sinc-Legendre [17]		Chebyshev [18]
	m=16	m=32	m=64	m=20	m=5	m=5	m=15	m=25
.1	2.7574e-10	6.093e-3	1.210e-3	1.369e-09	6.481e-04	6.994e-5	6.462e-6	7.964e-06
.2	1.1523e-10	4.843e-3	1.259e-3	7.591e-10	4.109e-04	1.721e-4	1.578e-5	3.912e-06
.3	1.0499e-10	2.750e-2	1.865e-3	1.184e-09	5.493e-04	2.472e-4	2.272e-5	6.162e-06
.4	4.4687e-09	1.937e-2	7.412e-3	1.068e-09	5.198e-04	2.912e-4	2.674e-5	5.953e-06
.5	1.4132e-09	1.000e-6	1.000e-6	9.819e-10	4.912e-04	3.004e-4	2.759e-5	2.103e-06
.6	1.0483e-09	4.359e-2	7.460e-3	1.039e-09	5.063e-04	2.760e-4	2.534e-5	7.639e-06
.7	1.1720e-09	1.734e-2	1.724e-3	1.031e-09	5.045e-04	2.213e-4	2.035e-5	1.967e-06
.8	2.8697e-09	7.750e-2	4.990-3	1.030e-09	5.040e-04	1.440e-4	1.320e-5	8.103e-06
.9	1.6423e-09	4.443e-2	1.678e-2	1.031e-09	5.037e-04	5.026e-5	4.653e-6	6.019e-06

The given problem has an exact solution provided below as:

$$x(\rho,\theta) = \left(1+\theta^{2\alpha}\right)\left(\rho-\rho^{3}\right). \tag{56}$$

In Figure 3A, we illustrate a comparison of the exact solution with the one derived using the Bell wavelet method. Figures 3B–D showcase approximate solutions behavior for various values of α. Additionally, Figure 3E graphically presents the absolute error. Tables 3, 4, and 5 compare the AE of our method with Chebyshev method for $\alpha = 0.7$, $\alpha = 0.9$, and $\alpha = 0.95$, respectively. These comparisons clearly demonstrate that the Bell wavelet method yields more accurate and precise results than those reported in [23].

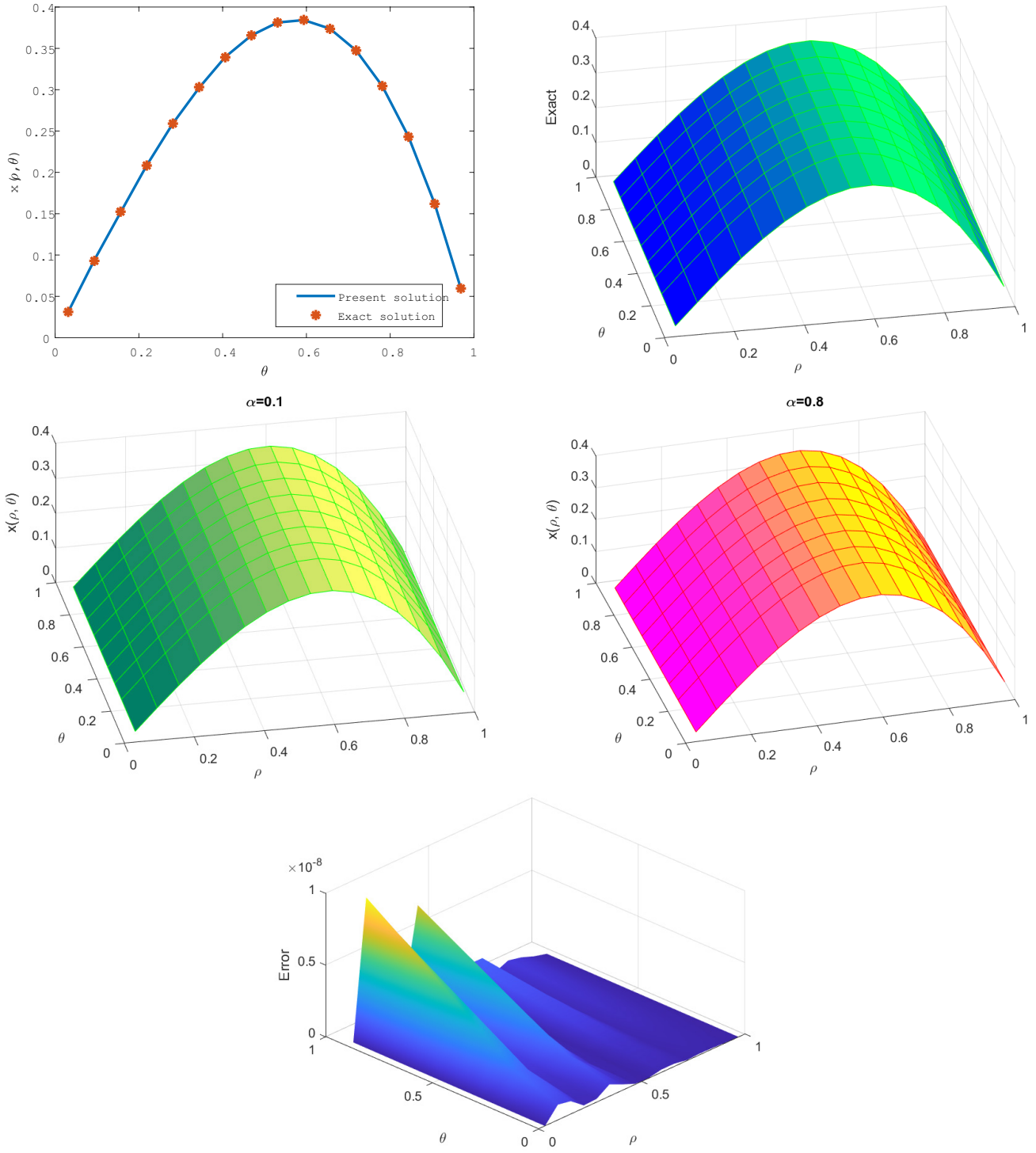

Figure 3: (A) 2D plot, (B,C) 3D Exact and approximate solutions respectively, (D) Approximate solution at different α=0.8 and (E) AE at α = 0.5 of Problem 6.6.

Table 3: AE of Problem 6.6 at $\alpha = 0.7,\ \rho = 0.1$.

ρ	Present method		Fibonacci method [30]		Chebyshev method [18]	
	k=2, M=3	k=3, M=4	m=6	m=16	m=5	m=6
.1	5.3268e-07	1.0658e-09	1.1756e-05	4.427e-05	3.0250e-03	3.0250e-03
.2	1.0790e-07	2.1588e-09	1.6749e-05	2.3162e-04	5.8161e-03	5.8222e-03
.3	9.0677e-07	1.8142e-09	2.2330e-05	1.1326e-04	8.1562e-03	8.1614e-03
.4	1.9498e-07	3.9011e-08	2.6343e-05	8.7111e-04	9.8378e-03	9.8394e-03
.5	2.3547e-07	4.7112e-08	3.0453e-04	5.0590e-05	1.0675e-02	1.0675e-02
.6	8.3519e-07	1.6710e-08	2.9697e-04	9.8069e-04	1.0492e-02	1.0492e-02
.7	4.1810e-07	8.3652e-09	1.8168e-04	2.9411e-04	9.3664e-03	9.3727e-03
.8	4.9919e-07	9.9884e-09	5.2042e-04	3.7305e-04	7.1335e-03	7.1396e-03
.9	1.3817e-07	2.7651e-08	3.2069e-04	1.2340e-04	3.9448e-03	3.9436e-03

Table 4: AE of Problem 6.6 at $\alpha = 0.9,\ \rho = 0.1$.

ρ	Present method		Fibonacci method [30]		Chebyshev method [18]	
	k=2, M=3	k=3, M=4	m=6	m=16	m=5	m=6
.1	1.5994e-07	2.1334e-08	1.9579e-05	2.3215e-05	2.4568e-03	2.4473e-03
.2	3.2394e-07	4.3208e-08	1.8181e-05	3.6568e-05	4.7198e-03	4.7146e-03
.3	2.7223e-07	3.6311e-08	2.1976e-05	2.0309e-05	6.6174e-03	6.6114e-03
.4	5.8537e-07	7.8078e-08	2.5772e-05	4.6186e-05	7.9816e-03	7.9728e-03
.5	7.0694e-07	9.4292e-08	6.3649e-05	8.7586e-05	8.6666e-03	8.6566e-03
.6	2.5074e-07	3.3445e-08	5.3649e-05	9.2855e-05	8.5616e-03	8.5537e-03
.7	1.2552e-07	1.6742e-08	4.3685e-05	2.9346e-05	7.6045e-03	7.5997e-03
.8	1.4989e-07	1.9994e-08	4.3685e-05	9.9165e-06	5.7951e-03	5.7900e-03
.9	4.1503e-07	5.5373e-08	6.7125e-05	2.4445e-06	3.2082e-03	3.1971e-03

Table 5: AE of Problem 6.6 at $\alpha = 0.95,\ \rho = 0.1$.

ρ	Present method		Fibonacci method [30]		Chebyshev method [18]	
	k=2, M=3	k=3, M=4	m=6	m=16	m=5	m=6
.1	2.6680e-07	3.2029e-09	1.6506e-05	9.9082e-05	2.3392e-03	2.3521e-03
.2	5.4030e-07	6.4860e-09	1.5170e-05	8.4734e-05	4.5017e-03	4.5138e-03
.3	4.5406e-07	5.4507e-08	1.5170e-05	9.9616e-05	6.3151e-03	6.3227e-03
.4	9.7633e-07	1.1720e-08	2.2340e-05	9.5819e-05	7.6190e-03	7.6213e-03
.5	1.1790e-07	1.4154e-08	4.3081e-05	8.4703e-05	8.2740e-03	8.2740e-03
.6	4.1822e-07	5.0205e-08	3.8961e-05	5.4591e-05	8.1741e-03	8.1765e-03
.7	2.0935e-07	2.5132e-08	3.0239e-05	7.3382e-06	7.2598e-03	7.2674e-03
.8	2.5004e-07	3.0018e-08	4.1836e-05	7.0254e-06	5.5306e-03	5.5422e-03
.9	6.9260e-07	8.3164e-08	4.4536e-05	8.3595e-07	03.0577e-03	3.0699e-03

Problem 6.7 *Consider the following α th order $(0<\alpha<1)$ TFCDE*

$$\frac{\partial^{\alpha}x(\rho,\theta)}{\partial\theta^{\alpha}}-\frac{\partial^{2}x(\rho,\theta)}{\partial\rho^{2}}=2\left(\frac{1}{\Gamma(3-\alpha)}\theta^{2-\alpha}-1\right),\quad 0<\rho<1,\quad 0<\theta\leq 1, \tag{57}$$

with conditions given below as:

$$x(0,\theta)=\theta^{2},\quad x(1,\theta)=1+\theta^{2},\quad x(\rho,0)=\rho^{2}, \tag{58}$$

Exact solution of (57) is

$$x(\rho,\theta)=\rho^{2}+\theta^{2}. \tag{59}$$

Figures 4A–C depict the comparison between the Bell wavelet solution and exact solution. The AE for $\alpha=0.75$ is shown in Figure 4D. Table 6 provides a comparison of the absolute error at $\alpha=0.5$ and $\rho=0.25$ between our approximated solution with BFM method [20], and the Fibonacci wavelet [32]. This comparison highlights the enhanced accuracy of our approach.

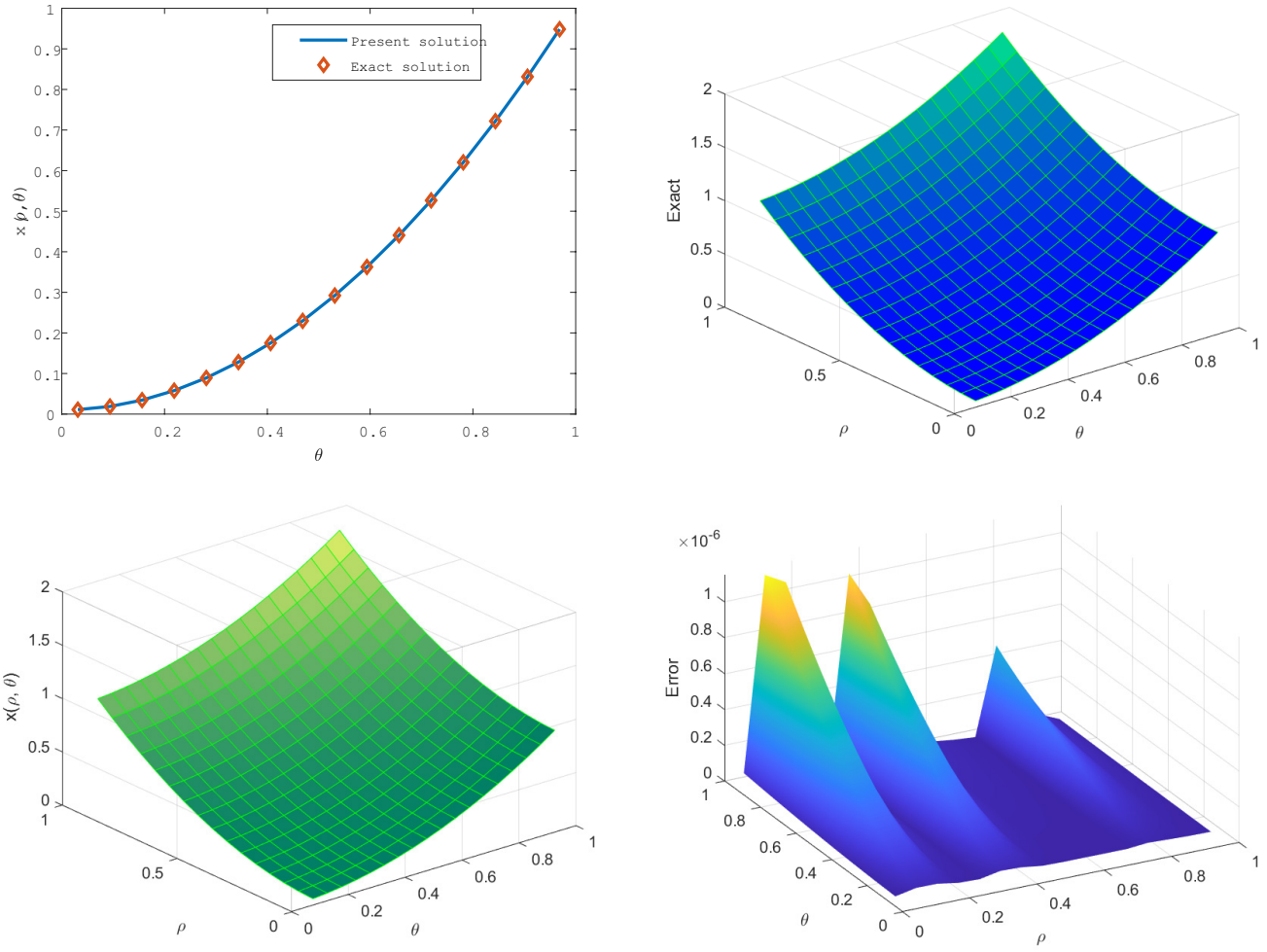

Figure 4: (A) 2D plot, (B,C) 3D Exact and approximate solutions respectively and (D) AE at $\alpha=0.5$ of Problem 6.7.

Table 6: AE of Problem 6.7 at $\alpha = 0.5$, $\rho = 0.25$.

ρ	Present method		Fibonacci method [30]		BFM [32]		
	k=2 M=3	k=3 M=4	k=2 M=3	k=3 M=4	j=1 m=2	j=2 m=2	j=1 m=3
.2	6.0548e-07	1.0554e-09	2.0561e-04	6.3909e-05	3.3e-2	8.8e-2	4.4e-3
.4	6.3099e-07	6.9669e-08	5.2032e-04	8.6140e-05	1.9e-2	9.8e-2	5.1e-2
.6	4.3249e-07	7.5519e-08	9.9285e-05	2.541e-04	1.6e-2	3.4e-1	7.1e-2
.8	3.4235e-07	3.3628e-08	9.9285e-05	5.6495e-07	1.2e-1	4.3e-1	2.8e-2

7. Conclusion

In this study, we successfully utilized the Bell wavelet collocation method to address TFCDEs. By constructing the OMI order using BPFs, we have converted the TFCDE to a system of algebraic equations, thereby enhancing convergence speed and reducing computational complexities compared to existing methods. Our comparative analysis against Fibonacci wavelet methods [30], BFM [32], Chebyshev method [18], Haar wavelet [31], and B-spline method [33] underscores the effectiveness and accuracy of proposed methodolgy. Moreover, our method demonstrates versatility in addressing both linear and nonlinear problems. The calculation of AEs for varying numbers of collocation points further solidifies the reliability of the Bell wavelet method. Overall, our approach stands out for its accuracy, flexibility, convenience, and computational efficiency, making it a highly effective solution for tackling complex problems in various fields.

Acknowledgement

We sincerely thank the reviewers for their insightful and valuable suggestions, which significantly improved this manuscript. Their suggestions, comments and recommendations are instrumental in improving the manuscript.

8. Declarations

Data availability

No data set was used in this study.

Declaration of competing interest

None.

References

[1] Podlubny I. Fractional differential equations: an introduction to fractional derivatives, fractional differential equations, to methods of their solution and some of their applications. elsevier; 1998.
[2] Kilbas AA, Srivastava HM, Trujillo JJ. Theory and applications of fractional differential equations. Elsevier; 2006.
[3] Miller KS, Ross B. An introduction to the fractional calculus and fractional differential equations. Wiley, New York. 1993 May.
[4] Machado JT, Kiryakova V, Mainardi F. Recent history of fractional calculus. Communications in nonlinear science and numerical simulation. 2011;16(3):1140-53.
[5] Das S. Functional Fractional Calculus for System Identification and Controls. Springer, New York 2008.
[6] He JH. Nonlinear oscillation with fractional derivative and its applications. InInternational conference on vibrating engineering. 1998; 98:288-291.
[7] Moaddy K, Momani S, Hashim I. The non-standard finite difference scheme for linear fractional PDEs in fluid mechanics. Computers & Mathematics with Applications. 2011;61(4):1209-16.
[8] Mainardi F. Fractional calculus: some basic problems in continuum and statistical mechanics. Springer Vienna; 1997.

[9] Grigorenko I, Grigorenko E. Chaotic dynamics of the fractional Lorenz system. Physical review letters. 2003;91(3):034101.
[10] Rossikhin YA, Shitikova MV. Applications of fractional calculus to dynamic problems of linear and nonlinear hereditary mechanics of solids. Applied Mechanics Reviews. 1997;50:15–67.
[11] Baillie RT. Long memory processes and fractional integration in econometrics. Journal of econometrics. 1996;73(1):5-9.
[12] Magin R. Fractional calculus in bioengineering, part 1. Critical Reviews™. Biomedical Engineering. 2004;32(1):1-104.
[13] Ahmed S, Jahan S, Nisar KS. Hybrid Fibonacci wavelet method to solve fractional-order logistic growth model. Mathematical Methods in the Applied Sciences. 2023;46(15):16218-31.
[14] Zhou F, Xu X. The third kind Chebyshev wavelets collocation method for solving the time-fractional convection diffusion equations with variable coefficients. Applied Mathematics and Computation. 2016;280:11-29.
[15] Biazar J, Asadi MA. Finite integration method with RBFs for solving time-fractional convection-diffusion equation with variable coefficients. Computational Methods for Differential Equations. 2019;7(1):1-5.
[16] Chen LJ, Li M, Xu Q. Sinc-Galerkin method for solving the time fractional convection–diffusion equation with variable coefficients. Advances in Difference Equations. 2020;2020(1):504.
[17] Saadatmandi A, Dehghan M, Azizi MR. The Sinc–Legendre collocation method for a class of fractional convection–diffusion equations with variable coefficients. Communications in Nonlinear Science and Numerical Simulation. 2012;17(11):4125-36.
[18] Saw V, Kumar S. The Chebyshev collocation method for a class of time fractional convection-diffusion equation with variable coefficients. Mathematical Methods in the Applied Sciences. 2021;44(8):6666-78.
[19] Uddin M, Haq S. RBFs approximation method for time fractional partial differential equations. Communications in Nonlinear Science and Numerical Simulation. 2011;16(11):4208-14.
[20] Jiang Y, Ma J. Moving finite element methods for time fractional partial differential equations. Science China Mathematics. 2013;56:1287-300.
[21] Xu X, Xu D. Legendre wavelets direct method for the numerical solution of time-fractional order telegraph equations. Mediterranean Journal of Mathematics. 2018;15:1-33.
[22] Cattani C. Harmonic wavelet solutions of the Schrodinger equation. International Journal of Fluid Mechanics Research. 2003;30(5).
[23] Ahmed S, Jahan S, Shah K, Abdeljawad T. On computational analysis via fibonacci wavelet method for investigating some physical problems. Journal of Applied Mathematics and Computing. 2024.
[24] Dehestani H, Ordokhani Y, Razzaghi M. Fractional-order Legendre–Laguerre functions and their applications in fractional partial differential equations. Applied Mathematics and Computation. 2018;336:433-53.
[25] Wang Y, Zhu L. Solving nonlinear Volterra integro-differential equations of fractional order by using Euler wavelet method. Advances in difference equations. 2017;2017:1-6.
[26] Canuto C, Hussaini MY, Quarteroni A, Zang TA. Spectral methods: fundamentals in single domains. Springer Science & Business Media; 2007.
[27] Ahmed S, Jahan S, Nisar KS. Haar Wavelet Collocation Method for Telegraph Equations with Different Boundary Conditions. Jordan Journal of Mathematics and Statistics. 2024;17(1):1-21.
[28] Wang Y, Zhou X. An Efficient Numerical Method Based on Bell Wavelets for Solving the Fractional Integro-Differential Equations with Weakly Singular Kernels. Fractal and Fractional. 2024;8(2):74.
[29] Yadav P, Jahan S, Nisar KS. A new generalized Bell wavelet and its applications for solving linear and nonlinear integral equations.Computational and Applied Mathematics. 2025;44(40).
[30] Yadav P, Jahan S, Nisar KS. Fibonacci wavelet method for time fractional convection–diffusion equations. Mathematical Methods in the Applied Sciences. 2024;47(4):2639-55.
[31] Chen Y, Wu Y, Cui Y, Wang Z, Jin D. Wavelet method for a class of fractional convection-diffusion equation with variable coefficients. Journal of computational science. 2010;1(3):146-9.
[32] Irandoust-pakchin S, Dehghan M, Abdi-mazraeh S, Lakestani M. Numerical solution for a class of fractional convection–diffusion equations using the flatlet oblique multiwavelets. Journal of Vibration and Control. 2014;20(6):913-24.
[33] Adibmanesha L, Rashidiniab J. Sinc and B-Spline scaling functions for time-fractional convection-diffusion equations. Journal of King Saud University-Science. 2021;33(2):101343.
[34] Yüzbaş, Ş. Fractional Bell collocation method for solving linear fractional integro-differential equations. Mathematical Sciences. 2024; 18(1), 29-40.
[35] Yüzbaş, Ş. A new Bell function approach to solve linear fractional differential equations. Applied Numerical Mathematics,2020; 174, 221-235.
[36] Yildiz, G., Tinaztepe, G., & Sezer, M. Bell polynomial approach for the solutions of Fredholm integrodifferential equations with variable coefficients. Computer Modeling in Engineering & Sciences. 2020; 123(3), 973-993.
[37] Yüzbaş, Ş. & Ismailov, N. (2018). An operational matrix method for solving linear Fredholm–Volterra integro-differential equations. Turkish Journal of Mathematics. 2018; 42(1), 243-256.
[38] Yüzbaş, Ş. & Ismailov, N. A Taylor operation method for solutions of generalized pantograph type delay differential equations. Turkish Journal of Mathematics.2018; 42(2), 395-406.
[39] Yüzbaş, Ş. An operational matrix method to solve the Lotka–Volterra predator–prey models with discrete delays. Chaos, Solitons & Fractals.2021; 153, 111482.